DATA ACQUISITION AND REDUCTION FOR THE UVA SUPERCONDUCTING MAGNETIC SUSPENSION AND BALANCE FACILITY[†]

by

I.D. Jacobson,[††] J.L. Junkins,[††] and J. R. Jancaitis[†††]
Department of Aerospace Engineering and Engineering Physics
University of Virginia

ABSTRACT

The problems associated with data acquisition and reduction in the U.Va. superconducting magnetic suspension and balance facility are similar to those in free-flight ranges (or tunnels). The model undergoes a "Quasi-six-degree-of-freedom" motion which must be monitored both in position and angular orientation from which the aerodynamics must be inferred. The data acquisition problem is made more difficult because geometric constraints prevent direct visual access to the model in the Mach 3 wind tunnel. The methods, accuracies and problems associated with the acquisition of data are discussed.

[†]This work was supported under NASA Grants 47-005-029, 149, 112

[††]Assistant Professor of Aerospace Engineering

[†††]Research Specialist

K.I.

1.0 Introduction

The problems associated with data reduction in the U.Va. superconducting magnetic suspension and balance facility (SMSB) are similar to those in free-flight ranges (or tunnels). A complete description of this facility can be found in reference 1. The model undergoes a "quasi-six-degree-of freedom" motion which must be monitored in both position and angular orientation, from which the aerodynamics must be inferred. The advantages of this facility over a conventional free flight facility is the ability to test over "long" times and gather more data, making the determination of model aerodynamics more accurate. In addition the increased length of time enables the transient part of the motion to decay allowing observation and analysis of steady-state motion. This promises to be a useful technique, as will be described below.

The precision with which we can determine the aerodynamics depends on two factors: first, the accuracy of the data acquisition technique used; and, second, the manner in which the errors propagate through the mathematical motion model and data reduction techniques. Here we will primarily be concerned with the latter; however, since it is an integral part of the data reduction scheme we will first discuss the data acquisition problem.

2.0 Data Acquisition

There are three methods for data acquisition in the U.Va. magnetic suspension facility. These are shown in Figures 1, 2, and 3. The first of these-the optical sensor (Figure 1), used to provide feedback for the control system, will also provide the primary data source for the data reduction process. The optical system is a conventional light beam-photocell system designed and calibrated to give position and angular data. The model geometry is one of the optical sensor design criteria, and hence, changing model geometry may require a new optical sensor design and calibration.

The optical system will hopefully be replaced by an electromagnetic sensor of the MIT type (Figure 2) which at this time is still under development. The main problems with the electromagnetic system arise from its use near a high alternating current source. The electromagnetic sensor will require less area in the annulus around the tunnel and thus allow a larger diameter test section. The primary motivation for development of the electromagnetic sensor is its invariance to model changes.[2]

The fiber optic system[3] (Figure 3) was designed primarily for use as a visual cue for the operator, who, due to the helium dewar, does not have a direct line of sight to the model. The distortion created (mostly barrel type), shown in Figure 4 can be compensated for by an extensive calibration procedure. This source of data is difficult to incorporate into the data reduction process since it requires a relatively large preprocessing effort and its estimated accuracy is an order of magnitude less than the other two systems as is illustrated in Table 1.

Table 1
Data Acquisition Systems Accuracies (estimates)

Sensor Type	Position	Angles
Optical	.1 mm (3 axes)	.05 degrees (2 planes)
Electromagnetic	.1 mm (3 axes)	.01 degrees (2 planes)
Fiber Optic	1 mm (3 axes)	.1 degree (1 plane)

3.0 Control Technique

In order to understand the concepts of data reduction as applied to

the model motion in the U.Va. magnetic suspension facility it is first necessary to understand the "quasi-six-degree-of-freedom" nature of the motion. By "quasi-six-degree-of-freedom" we mean the model is free to both rotate and translate at frequencies above some cutoff imposed by the SMSB control system. The feedback controller is designed to control only low frequency (O(10 hz)) and DC components of the model motion leaving the high frequency motion "untouched".

The maximum excursion of the model from the tunnel centerline at high frequencies given by

$$d_{max} = \frac{\alpha_{max} I_z}{m\ell} \qquad (3.0\text{-}1)$$

where α_{max} is the maximum angle of attack, I_z the pitch moment of inertia, m, the mass, and ℓ the distance between center of pressure and center of gravity.

For a typical model with a natural aerodynamic frequency of 35 hz the maximum displacement can be kept within 1 cm of the centerline.

In principle a controller which will leave the model aerodynamics "untouched" (i.e. not affect the roots of the characteristic equation associated with the aerodynamics) can be designed. It is one that requires feedback in position, velocity, angle and angular rate, the gains of each being determined by the method of Bass and Gura.[4] This method requires the knowledge of the aerodynamic properties of the model a priori, and freedom to use feedback in all the problem variables. Although feasible, this method is less desirable than a simple position-velocity controller.

An analysis of a simple position-velocity controller with a 3 hz natural frequency and $\sqrt{2}$ damping ratio has been carried out based on rather crude estimates of model aerodynamics. The indications are that there is little, if any, interaction with the model motion due to aerodynamics.

Two sources of error were examined:

1. Errors due to uncertainties in model aerodynamics.
2. Errors due to uncertainties in the position of the magnetic center with respect to the center of mass.

As can be seen from Figure 5 there is an insignificant effect on the damped natural frequency of the model and a small effect (about 2%) on the damping exponent. The error introduced by the controller into the damping exponent can easily be calibrated with wind off and used to compensate the later results of the inversion process to obtain aerodynamics. For the steady-state case a frequency response analysis for a typical model with and without controller was conducted. The results are given in Table II.

Table II
Frequency Response Analysis

Driving Frequency (Rad/Sec)	$\lvert\Delta/M_{ext}\rvert$ (Rad/Ft-lb)		$\lvert X/M_{ext}\rvert$ (Cm/Ft-lb)	
	Free	Controlled	Free	Controlled
150	1.56036	1.56981	17.4107	17.5269
175	1.91601	1.92581	15.7085	15.7964
200	2.45552	2.46566	15.4143	15.4838
225	2.96322	2.96845	14.698	14.7285
250	2.65051	2.64787	10.6494	10.6414
275	1.88953	1.88687	6.27438	6.26686
300	1.33748	1.33608	3.73196	3.7287

The conclusions to be drawn from the effects of the controller on the characteristic equation and the frequency response of the model are as follows:

1. For transient analyses the damping exponent may be affect by some small percentage (about 2-5%). This can be compensated for a posteriori.
2. There is insignificant effect on the frequency.
3. The forced steady-state motion is essentially unaffected by the controller.

Thus for the analysis of aerodynamics discussed in the next sections the model will be considered to be in free-flight with no inputs due to the feedback control system. This, it is felt, is the unique feature of this wind tunnel system - "long term" free-flight data.

4.0 Mathematical Models

4.0.1 The first mathematical model to be considered is well known linearized equations for a rolling missile with trigonal or greater symmetry[5]

$$[2\mu D - C_{z_\alpha} - C_{z_{\dot\alpha}} D - i\hat{p}_o(C_{z_{p\beta}} + C_{z_{p\dot\beta}} D)]A - [2\mu + C_{z_q} - i\hat{p}_o C_{z_{pr}}]D\Delta = F_{ext} \quad (4.0.1\text{-}1)$$

$$-[C_{m_\alpha} + C_{m_{\dot\alpha}} D + i\hat{p}_o(C_{m_{p\dot\beta}} D)]A + [i_B D^2 - C_{m_q} - i\hat{p}_o(i_A - C_{m_{pr}})]D\Delta = M_{ext} \quad (4.0.1\text{-}2)$$

where the C's are the aerodynamic coefficients, μ the nondimensional mass, i_A and i_B nondimensional inertias, $\hat{p}_o$ the nondimensional roll rate, D the derivative operator, A the complex angle of attack, Δ the complex orientation angle, F_{ext} and M_{ext} external driving functions. These equations have the familiar quadricyclic solution for either of the variables A or Δ, e.g.

$$\Delta = K_1 e^{(\lambda_1 + i\omega_1)t} + K_2 e^{(\lambda_2 + i\omega_2)t} + K_3 e^{i\omega_3 t} + K_4 \quad (4.0.1\text{-}3)$$

where K_i is the initial amplitude of the mode, λ_i is the damping rate of the mode, ω_i is the frequency of the mode, and ϕ_i is the phase angle of the mode. The subscripts 1, 2, 3, and 4 refer to the precession, nutation, rolling trim, and nonrolling trim modes respectively.

The constants K_i, λ_i, ω_i, and ϕ_i contain the information needed to obtain the aerodynamic coefficients. The precision to which the coefficients can be determined depends on the precision to which the data is known; examples of this will be given below.

Equation 4.0.1-3 contains the information needed to fit both transient (all four modes of motion) and steady-state (just the K3 and K4 modes of motion) data. The inversion process for transient case yields the aerodynamics in one run using the following relationships

$$C_{m_\alpha} = (\omega_1\omega_2 - \lambda_1\lambda_2)2I_y/\rho U^2 Sd \quad (4.0.1\text{-}4)$$

$$C_{mq} + C_{m_{\dot\alpha}} = [(\lambda_1 + \lambda_2) + \frac{\rho US}{2m}(-C_{z_\alpha} - C_D)]4I_y/\rho USd^2 \quad (4.0.1\text{-}5)$$

$$C_{m_{p\beta}} = [\frac{\omega_1\lambda_2 + \omega_2\lambda_1}{\omega_1 + \omega_2} + \frac{\rho US}{2m}(-C_{z_\alpha} - C_D)]4I_x/\rho USd^2 \quad (4.0.1\text{-}6)$$

where the drag coefficient and lift curve slope must be obtained by other means. The drag coefficient, C_D, determination is straightforward - being proportional to the force required to prevent the model from moving along

the tunnel axis. This force is easily determined to a high level of accuracy from the currents in the coils. The slope of the lift coefficient, C_{z_α} (as well as other translational aerodynamics) can be obtained from a standard swerve reduction program[5] (proportional to the lateral distance traveled).

The useful part of the application of the quadricyclic solution to both transient and steady-state data lies in the ability to write either the real or imaginary part of the solution; e.g.

$$\beta = Re(\Delta) = K_1\cos(\omega_1 t + \phi_1) + K_2\cos(\omega_2 t + \phi_2) + K_3\cos\omega_3 t + Re(K_4) \quad (4.0.1\text{-}7)$$

and still have all the information contained. This enables the application of the techniques indicated to data from a single plane.

4.0.2 The second model to be considered is the fitting of the observations to the equations of motion using a technique which we will call the "Brute-Force" method.[7] For an axisymmetric model only the z force and M pitching moment equations are necessary for the inversion; however, data on all kinematic variables is needed:

$$wC_{z_w} + qC_{z_q} + pvC_{z_{pv}} + DwC_{z_{Dw}} + pDvC_{z_{pDv}} + prC_{z_{pr}} = \mu(Dw - qu + pv) \quad (4.0.2\text{-}1)$$

$$wC_{m_w} + qC_{m_q} + pvC_{m_{pv}} + DwC_{m_{Dw}} + pDvC_{m_{pDv}} + prC_{m_{pr}} = i_B Dq - (i_C - i_A)pr + i_E(p^2 - r^2) - i_F(qr - Dp) + i_D(qp - Dr) \quad (4.0.2\text{-}2)$$

where v, w, p, q, r are the nondimensional kinematic velocities and the i's are moments and products of inertia. This model is fitted by reduction to a set of algebraic equations as described below.

4.0.3 The third model is a specialization of the first one (eq. 4.0.1-2) Here only steady-state motion is considered, perhaps the most unique model for[2] free flight facility to be using. The advantage to steady-state reduction is, of course, the increased accuracy to which the data can be determined, having many cycles of data to "smooth" over.

4.0.4 The last model considered is the full six degree of freedom equations of motion given in reference 5. Here the motion is allowed to include nonlinear aerodynamics as well as nonlinear inertia terms.

5.0 Data Reduction Techniques

Three conceptually different classes of methods have been investigated for extracting aerodynamics from available observations. These three classes are referred to here as

1. Differential Correction Methods,
2. "Brute Force" Method, and
3. Steady State Analysis Method.

Most conventional procedures belong to class (1). Our particular adaptations are in some aspects unique, as will be explained below, but in general represent the state-of-the-art of this approach. Classes (2) and (3) are original approaches growing out of our research efforts at U.Va.

5.0.1 Differential Correction Methods

Here we are referring to the class of numerical methods which successively improve preliminary values for the unknown parameters in a given mathematical model until the computed output agrees with observations in some optimum sense (in our case, minimizing the weighted sum of squares of observed-minus-computed residuals). We have employed two differential

correction formulations in our data reduction analyses, these are

$$\Delta P = (A^T W A)^{-1} A^T W \Delta \Psi, \qquad (5.0.1\text{-}1)$$

and

$$\Delta P = -\left(\frac{\Delta C}{G^T G}\right)^{1/2} G \qquad (5.0.1\text{-}2)$$

where

$$\Delta P \equiv n \times 1 \text{ matrix of corrections to parameters,} \qquad (5.0.1\text{-}3)$$

$$\Delta \Psi \equiv m \times 1 \text{ matrix of observation residuals,} \qquad (5.0.1\text{-}4)$$

$$A \equiv m \times n \text{ Jacobian matrix of partial derivatives of the } m \text{ observables with respect to the } n \text{ parameters, evaluated with the current parameter estimates,} \qquad (5.0.1\text{-}5)$$

$$W \equiv m \times m \text{ weighting matrix,} \qquad (5.0.1\text{-}6)$$

$$\phi \equiv \Delta \Psi^T W \Delta \Psi, \qquad (5.0.1\text{-}7)$$

$$G^T \equiv \left[\frac{\partial \phi}{\partial p_1}\Big|_c \cdots \frac{\partial \phi}{\partial p_n}\Big|_c\right] \qquad (5.0.1\text{-}8)$$

and

$$\Delta C \equiv \Delta P^T \Delta P, \ \Delta C \text{ assigned empirically.} \qquad (5.0.1\text{-}9)$$

The reader is referred to reference 8 for theoretical derivations and discussions of (5.0.1-1) and (5.0.1-2).

The first differential correction formula (5.0.1-1) is the classic least squares solution. The second formula (5.0.1-2) is the method of gradients ("steepest descent") solution for minimizing an arbitrary function.

Evaluation of the derivative matrix (5.0.1-5) is often a source of numerical difficulty. For analytic algebraic observation equations, we have developed, and used extensively a computer program which completely automates the process of partial differentiation. This process was employed with the quadricyclic solution as given in 4.0.1. For those cases in which the full six-degree-of-freedom equations (4.0.4) were integrated, we adopted a process known as parametric differentiation for computation of the elements of the observation Jacobian (5.0.1-5). This procedure[8] develops a set of m x n differential equations (one for each element of A) which can be integrated simultaneously with the equations of motion. These equations follow from straight forward partial differentiation of the equations of motion.

Comparing the method of gradients correction equation (5.0.1-2) with the least square correction equation (5.0.1-1), we note that use of (5.0.1-2) eliminates the necessity of inverting $(A^T W A)$, but introduces the necessity of controlling convergence rate by logically assigning ΔC (5.0.1-9) in (5.0.1-2). Our experience indicates that (5.0.1-2) is a valid alternative to (5.0.1-1), but should be employed only in the event that $(A^T W A)$ is so poorly conditioned that numerical inversion is impossible. We have found that the classical least square solution is typically an order of magnitude more efficient as the basis for least square differential corrections.

5.0.2 The "Brute Force" Method

Equations 4.0.1-1, 2 are solvable by differentiating the data numerically (using a five point central differencing scheme) and assuming all the observable kinematics to be known quantities. Thus the equations of motion are reduced to a set of linear algebraic equations in the aerodynamics which can be inverted to obtain the aerodynamics. As one might suspect, the accuracy of this method is highly sensitive to errors in observed data, since

numerical differentiation is being performed. This method also requires data on both position and angles in two orthogonal planes, however it is capable of handling a more sophisticated (i.e. nonlinear) model of the aerodynamic forces and moments.

For more details on this "Brute Force" method see reference 7. Comparison of this method with the others will be presented below.

5.0.3 Steady-State Analysis

5.0.3.1 Equations

As stated before, the coupled, complex, second order, linear differential equations which describe the motion of our model reduce to two complex algebraic equations when only the steady-state response is considered.

The resulting equations can be arranged[9] in the following fashion:

$$\text{Real} \quad \left(\frac{2\mu i\omega\Delta_o}{A_o}\right) \doteq [\hat{p}_o(C_{z_{pr}} + C_{z_{p\dot{\beta}}})]\omega + [C_{z_\alpha}] \qquad (5.0.3.1\text{-}1)$$

$$\text{Imag} \quad \left(\frac{2\mu i\omega\Delta_o}{A_o}\right) \doteq [-(C_{z_{\dot{\alpha}}} + C_{z_q})]\omega + [-\hat{p}_o C_{z_{p\beta}}] \qquad (5.0.3.1\text{-}2)$$

$$\text{Real} \quad \left(\frac{M}{A_o}\right) \doteq [-i_B]\omega^2 + [\hat{p}_o i_A]\omega + [-C_{m_\alpha}] \qquad (5.0.3.1\text{-}3)$$

$$\text{Imag} \quad \left(\frac{M_o}{A_o}\right) + \frac{C_{z_\alpha}}{2\mu}(i_A\hat{p}_o - i_B\omega) \doteq [-(C_{m_q} + C_{m_{\dot{\alpha}}})]\omega + [-C_{m_{p\beta}}\hat{p}_o] \qquad (5.0.3.1\text{-}4)$$

The terms appearing on the left hand side of the equations are all observables (or in the case of the last equation - computable before they are needed). These quantities are determined for each of several frequencies on the frequency response curve. Due to the periodic non-damped nature of the steady state solution Δ_o and A_o can be determined using a simple least square procedure or fourier analysis to obtain amplitude, phases, and frequencies. Since a linear model has been assumed, observations of one plane of data (both angle and velocity) is sufficient. Each of the first four equations are valid for the n-points used on the frequency response curves. Therefore, we have n sets of equations whose solution is a simple non-iterative least squares reduction for the coefficients.

The major advantages of this method are its simplicity (no interation necessary) and its relative insensitivity to reasonable measurement errors.

The determinable coefficients include all of the coefficients on the right hand side of equations 5.0.3.1-1, 2, 3 and 4. This, it should be noted, includes inertia terms.

5.0.3.2 Magnetic Investigation of Resonance

In the steady state case the use of an oblate spheroid for the support element will also allow for an investigation of a resonance curve. In the previous section this was shown to be sufficient to determine the models aerodynamics. Use of an oblate spheroid provides an additional "spring constant" term (which is proportional to the magnitude of the main field) in the rotational equation of motion.

For discussion's here we assume no translation, the models motion is given by:

$$\{-[C_{m_\alpha} + C_{m_{\Delta_{BAL}}} + C_{m_{\dot\alpha}} D + i\hat{p}_o (C_{m_{p\dot\beta}} D)] + I_B D^2 - C_{m_q} D - i\hat{p}_o (I_A D - C_{m_{pr}} D)\} = M_o e^{i\omega\hat{t}} \quad (5.0.3.2\text{-}1)$$

Assuming the steady state solution ($\Delta = \Delta_o e^{i\omega\hat{t}}$ and for simplicity assume $\hat{p}_o = 0$, then rearranging and separating the equation into real and imaginary parts;

$$\text{Real}\left(\frac{M_o}{\Delta_o}\right) = -C_{m_{\Delta_{BAL}}} + [-I_B\omega^2 - C_{m_\alpha}] \quad (5.0.3.2\text{-}2)$$

$$\text{Imag}\left(\frac{M_o}{\Delta_o}\right) = (C_{m_q} + C_{m_{\dot\alpha}})\omega \quad (5.0.3.2\text{-}3)$$

For numerous runs, all with the same ω but different $C_{m_{\Delta_{BAL}}}$ the problem becomes the same as that described in the previous section. It should be noted that the "variable" is now $C_{m_{\Delta_{BAL}}}$ not "ω" as before.

This method will be investigated numerically in the near future, no results are as yet available.

A disadvantage of this method that is that the translation equation of motion is unchanged. All the quantities appearing are constant, making it necessary to vary ω (as well as $C_{m_{\Delta_{BAL}}}$) to evaluate all of the aerodynamic coefficients involved.

6.0 Numerical Results

A comparative numerical study of how observational statistics propagate through the data reduction methods into statistics of the determined aerodynamic derivatives has been carried out. Observations were simulated by corrupting perfect (computed) values of the observables by adding Gaussian random relative errors. Several noise samples were taken at each noise level (σ); and each of the several applicable data reduction techniques were employed to determine the corresponding values for the aerodynamic derivatives. From these results, small sample statistics of the determined derivatives were computed for each method. Typical results of these analyses are displayed in figures 6, 7, 8 and 9 for a 15° included angle cone.

All the data are presented as percent standard deviation of the aerodynamic coefficients versus percent random noise† superimposed on the data. The major observation to be made is the consistent superiority of the steady-state method over the others. The translational derivatives (not shown) follow the same pattern with the steady-state method yielding the most accurate inversion at a given noise level. The errors noted in the differential correction methods are approximately the same as other investigators using these methods have found them to be.

One interesting fact to be reported on in detail in a future publication is the ability to separate C_{m_q} and $C_{m_{\dot\alpha}}$ for reasonable noise levels using the "Brute Force" method.

† Curves 1 and 2 have a slightly higher positional noise level than the others, however our experience indicates that the moment coefficients are not extremely sensitive to positional noise.

7.0 Conclusions

An analysis of several methods for obtaining aerodynamic coefficients from the U.Va. superconducting magnetic suspension and balance wind tunnel system has been carried out. The method for inverting steady state free-flight motion yields more precise aerodynamic coefficients than transient methods at the same measurement noise level.

References

1. Zapata, R. N., Paper A, This conference proceedings.
2. Stephens, T. "The Electromagnetic Position Sensing System", Paper G, This conference proceedings.
3. Lapins, M. "Optical Data Acquisition for the Cold Magnetic Balance Wind Tunnel Facility" Masters Thesis UVA June 1970.
4. Bass, R. W., and Gura, I. "High Order System Design Via State Space Considerations" Preprint, JACC Conference, Troy, N.Y. June 1965 p. 311-318.
5. Etkin, B. Dynamics of Flight, John Wiley and Sons, Inc. 1959.
6. Murphy, C. H. Free Flight Motion of Symmetric Missiles," BRL Rept No. 1216, July 1963.
7. Ragunath, B. S. "Error Analysis in the Evaluation of Aerodynamic Derivatives from University of Virginia Wind Tunnel Cold Magneitc Balance System." Ph.D. Dissertation UVA, June 1971.
8. Junkins, J. L. "On the Determination and Optimization of Powered Space Vehicle Trajectories Using Parametric Differential Correction Processes" MDC Rept No. G1793, 1969.
9. Jancaitis, J. R. "Steady-State Data Reduction Technique for UVA Cold Magnetic Balance System" Unpublished UVA Report 1971.

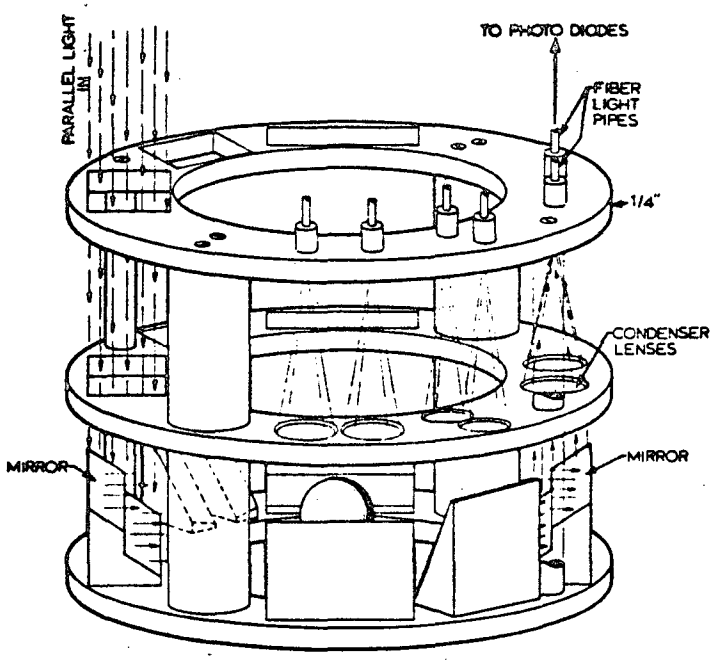

Figure 1 Optical Sensing System

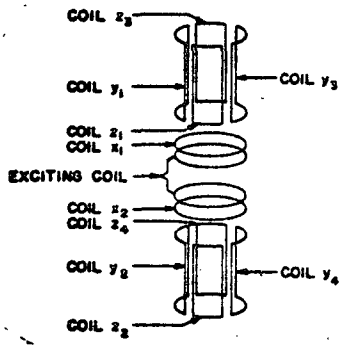

Figure 2 Electromagnetic Sensing System

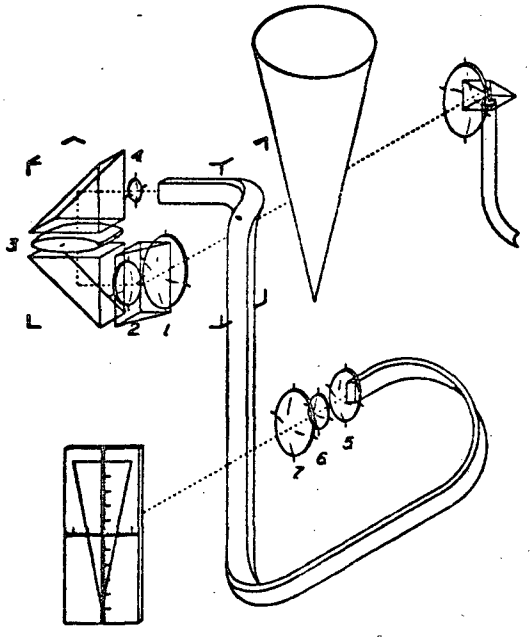

Figure 3 Fiber Optic System

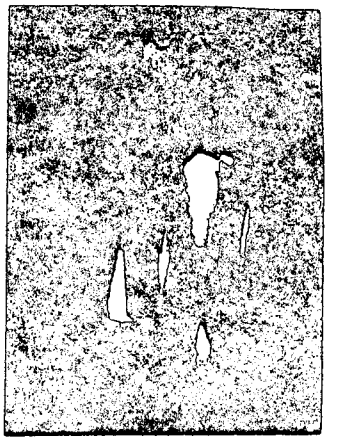

Figure 4 Distorted Cone

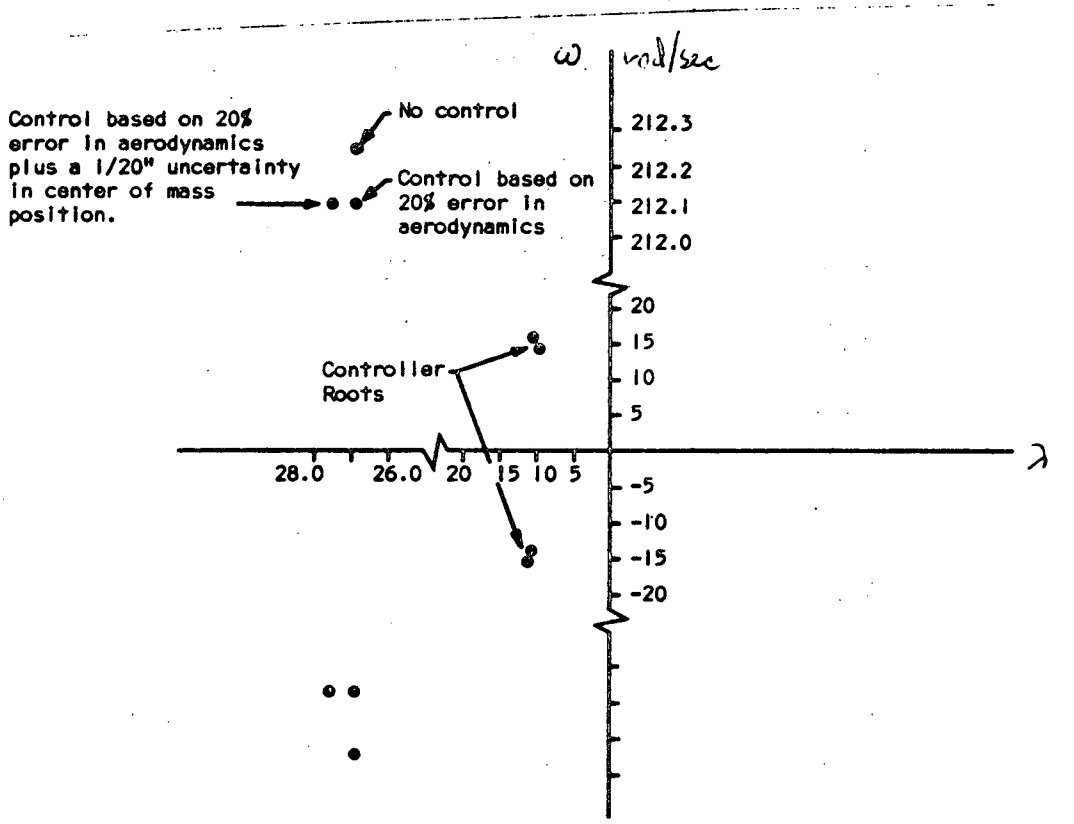

Figure 5 Root Locus of Model Aerodynamics

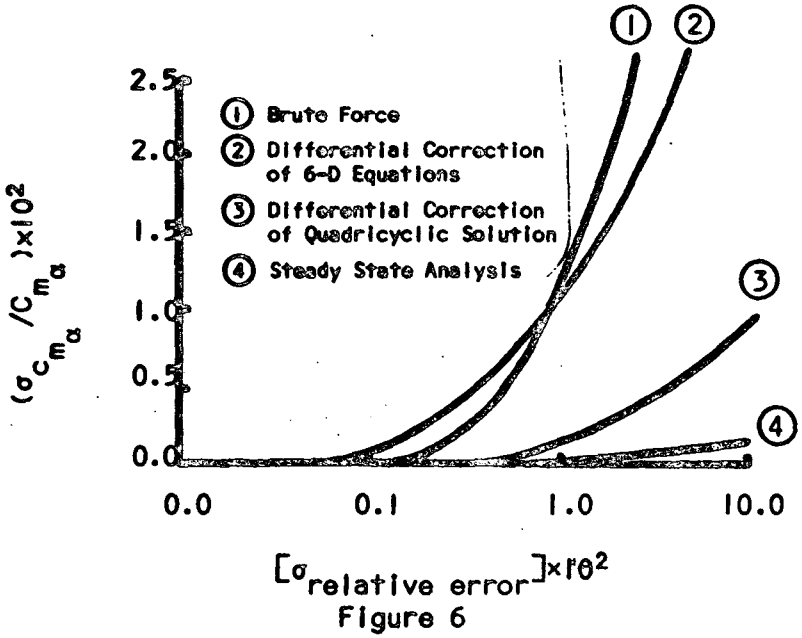

Figure 6

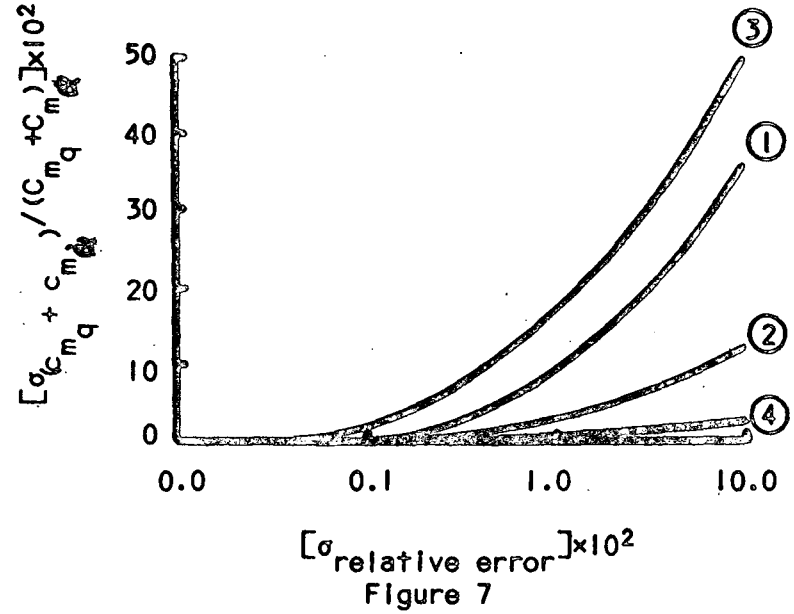

Figure 7

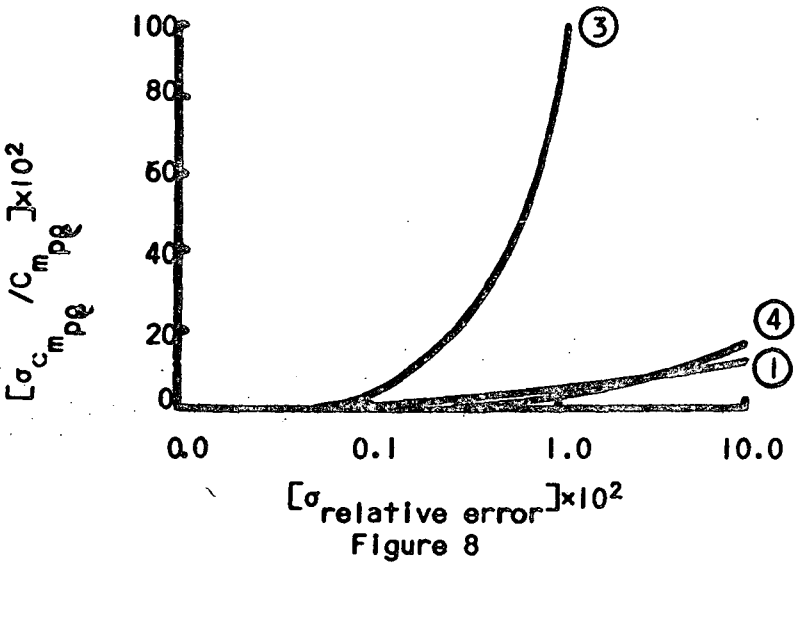

Figure 8

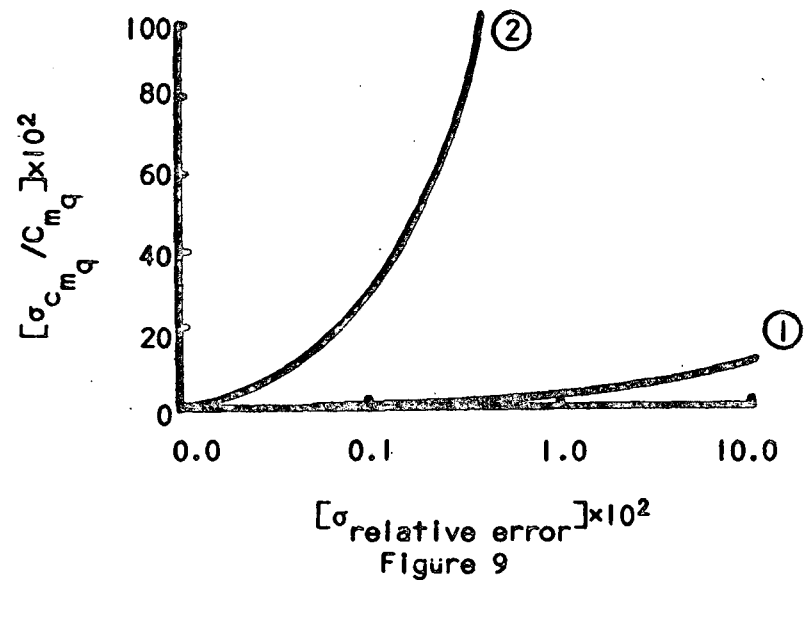

Figure 9